NIH Public Access
Author Manuscript
Nanoscale. Author manuscript; available in PMC 2014 April 21.

Published in final edited form as:
Nanoscale. 2013 April 21; 5(8): . doi:10.1039/c3nr34152f.

Polarization properties of fluorescent BSA protected Au_{25} nanoclusters

Sangram Raut[a], **Rahul Chib**[a], **Ryan Rich**[a], **Dmytro Shumilov**[b], **Zygmunt Gryczynski**[a,b], and **Ignacy Gryczynski**[a,c]

[a]Center for Commercialization of Fluorescence Technologies, Department of Molecular Biology and immunology, University of North Texas Health Science Center, 3500 Camp Bowie Blvd. Fort Worth, Texas, USA, 76107.

[b]Department of Physics. Texas Christian University, 2800 S. University Dr., Fort Worth, Texas, USA, 76129.

[c]Department of Cell Biology and Anatomy, University of North Texas Health Science Center. 3500 Camp Bowie Blvd. Fort Worth, Texas, USA, 76107.

Abstract

BSA protected gold nanoclusters (Au_{25}) are attracting great deal of attention due to their unique spectroscopic properties and possible use in biophysical applications. Although there are reports on synthetic strategies, spectroscopy and applications, little is known about their polarization behavior. In this study, we synthesized the BSA protected Au_{25} nanoclusters and studied their steady state and time resolved fluorescence properties including polarization behavior in different solvents: glycerol, propylene glycol and water. We demonstrated that the nanocluster absorption can be separated from the extinction spectrum by subtraction of Rayleigh scattering. The nanocluster absorption spectrum is well approximated by three Gaussian components. By a comparison of the emissions from BSA Au_{25} clusters and rhodamine B in water, we estimated the quantum yield of nanoclusters to be higher than 0.06. The fluorescence lifetime of the BSA Au_{25} cluster is long and heterogeneous with an average value of 1.84 μs. In glycerol at −20°C the anisotropy is high, reaching a value of 0.35. However, the excitation anisotropy strongly depends on the excitation wavelengths indicating a significant overlap of the different transition moments. The anisotropy decay in water reveals a correlation time below 0.2 μs. In propylene glycol the measured correlation time is longer and initial anisotropy depends on the excitation wavelength. The BSA Au_{25} cluster, due to long lifetime and high polarization, can potentially be used in studying large macromolecules such as protein complexes with large molecular weight.

Introduction

Metal nanoclusters (Au, Ag and Cu) hold great promise in terms of biophysical applications due to their unique fluorescence properties [1, 2]. These metal nanoclusters can be used in a variety of disciplines including but not limited to catalysis, biosensing, photonics, and molecular electronics[3-6]. The metallic clusters range in size less than 2 nm, which is comparable to the Fermi wavelength of electrons, and they bridge the gap between the behavior of metal atoms and metal nanoparticles. Owing to their small size, they do not sustain collective plasmon oscillations and are unable to support Surface Plasmon Resonance (SPR). Therefore their properties differ significantly from plasmonic nanostructures. Recently nanoclusters have been synthesized with precise control over the number of atoms in the metal core, which subsequently achieved the desired emission wavelength[7,8]. Different types of capping ligands ranging from small molecules like

NIH-PA Author Manuscript
NIH-PA Author Manuscript
NIH-PA Author Manuscript

NIH-PA Author Manuscript

NIH-PA Author Manuscript

NIH-PA Author Manuscript

glutathione to large molecular weight proteins such as BSA have been utilized to synthesize these clusters.

Protein-stabilized Au nanoclusters (Au NC) are receiving attention from the scientific community for their strong and tunable fluorescence in the visible spectrum. Xie *et al.* used BSA when they introduced a facile protein directed synthesis, which was followed by many research groups for other protein- Au NC systems [9]. Recently, different proteins have been used as a template to synthesize fluorescent metal nanoclusters. Specifically for Au NC, different investigators have used BSA, HSA, lysozyme, trypsin and the ferritin family of proteins [10-13]. Different ligands produce clusters with varying absorption and emission properties due to the different number of atoms present in the metal cluster core. There are several reports on the spectroscopic behavior of Au NC, and some of them have been mentioned below in order to understand the mechanism of luminescence and ligand-metal core interactions.

Sakanaga *et al.* reported the excited energy emission bands of the Au_{25} nanocluster and isolated two luminescence transitions, one band between 6sp states and other excited state band between 6sp and 5d states [14]. Furthermore, Jin *et al.* synthesized the Au_{25} clusters stabilized with different ligands and showed the trend of increasing fluorescence intensity due to the ligand's ability to donate electron density to the Au NC surface [15]. Wen *et al.* demonstrated that BSA-protected Au_{25} NCs consist of prompt fluorescence in the nanosecond time scale and delayed fluorescence in the microsecond time scale [16]. Their findings suggest that delayed fluorescence dominates the red band due to efficient intersystem crossings owing to the very small energy gap between the singlet and the triplet states. Moreover, another publication from Wen *et al.*, showed that fluorescence from BSA Au_{25} clusters is consists of two luminescence bands, one at 710 nm (band I) and one at 640 nm (band II)[17]. The temperature dependence study shows that band I originates from the metal core, whereas band II arises due to metal core-ligand interaction. These reports suggest that we do have reasonable understanding of the origin of absorption and luminescence from BSA Au_{25} clusters.

Despite the number of publications as cited above on the BSA Au_{25} clusters ranging from synthetic strategies, spectroscopic, electronic behavior and biochemical applications, there are no reports on the polarization properties of these protein protected Au clusters. In this manuscript we have studied BSA Au_{25} clusters' steady state and time resolved fluorescence and polarization behavior in water, propylene glycol and glycerol. The objective of the current work is to show that BSA Au clusters show polarization behavior despite long fluorescence lifetime which can be explored to our advantage in terms of developing polarization based sensing applications.

Experimental Section

Synthesis of BSA Au_{25} nanoclusters

The Au_{25} NCs used in this study were synthesized using an approach developed by Xie *et al.*[9]. Typically, 5 mL of 10 mM $HAuCl_4$ was mixed with 5 mL of 50 mg/mL BSA followed by addition of 1mL 1M NaOH and kept at 37 °C overnight in the incubator. The light brown solution of clusters was further dialyzed (2000 MWCO membrane) against de-ionized water for at least 12 hr with periodic change of water to remove any small impurities. Dialyzed cluster solution was filtered using 0.02μm syringe filter and used for subsequent measurements.

NIH-PA Author Manuscript
NIH-PA Author Manuscript
NIH-PA Author Manuscript

Spectroscopic measurements

UV-Vis absorption and fluorescence spectra were obtained using a Cary 50 bio UV–visible Spectrophotometer (Varian Inc.) and Cary Eclipse Spectrofluorometer (Varian Inc.) respectively. All the measurements were done in 1cm X 1cm cuvettes at room temperature with optical density below 0.05 unless mentioned otherwise. In order to measure the quantum yield, corrected absorption spectra of BSA Au_{25} were collected by subtracting the scattering component from BSA Au_{25} absorption spectra followed by measuring the integrated fluorescence intensity of the Au_{25} nanoclusters. A solution of rhodamine B in ethanol (quantum yield: 0.7) was used as a reference [18]. The samples for anisotropy measurements were prepared using concentrated cluster stock solution in water. Amount of water in glycerol and propylene glycol was kept below 10% by volume. For steady state emission anisotropy, the sample was excited using 590 nm and emission was scanned from 610 nm to 800 nm using a 610 long wavelength pass filter and manually operated parallel and perpendicular polarizers. For steady state excitation anisotropy, emission was observed at 700 nm and excitation was scanned from 320 nm to 620 nm, using a 320 long pass filter on excitation and a 610 long pass filter on the emission side. The G factor was measured and incorporated in the anisotropy calculation using the following formula;

$$r = \frac{I_{VV} - GI_{VH}}{I_{VV} + 2GI_{VH}} \quad (1)$$

Where, I_{vv} is fluorescence intensity in parallel polarizer orientation, I_{VH} is fluorescence intensity in perpendicular orientation of polarizer's and G is a instrumental correction factor. Time resolved anisotropy and fluorescence lifetime was measured on a FluoTime 300 fluorometer (PicoQuant, Inc.) using a Fianium laser with tunable excitation. The fluorometer is equipped with an ultrafast microchannel plate detector (MCP) from Hamamatsu, Inc. The fluorescence lifetimes were measured in the magic angle condition and data analyzed using FluoFit4 program from PicoQuant, Inc (Germany) using multi-exponential fitting model;

$$I(t) = \sum_i \alpha_i e^{-t/\tau_i} \quad (2)$$

Where, α_i is the amplitude of the decay of the *i*th component at time t and τ_i is the lifetime of the *i*th component. The intensity weighted average lifetime (τ_{Avg}) was calculated using following equation;

$$\tau_{avg} = \sum_i f_i \tau_i \text{ Where, } f_i = \frac{\alpha_i \tau_i}{\sum_i \alpha_i \tau_i} \quad (3)$$

Excitations used for time resolved anisotropy measurements were 600 nm, 550 nm and 480 nm, while emission was observed at 700 nm with vertical and horizontal polarizer position on emission side using appropriate filters on both excitation and emission side. Anisotropy decays were analyzed with a bi-exponential fitting model in the FluoFit4 program from PicoQuant, Inc (Germany) using the following equation;

$$r(t) = \sum_i r_i e^{-t/\Phi_i} \quad (4)$$

Where, r_i is the anisotropy of the *i*th component at time t and Φ_i is the rotational correlation time of the *i*th component. The quality of the fit in lifetime and anisotropy decay analysis was judged by the chi square value and by the quality and autocorrelation of the residuals. The hydrodynamic particle size of BSA Au_{25} clusters was measured using a Nanotrac system (Mircotrac, Inc., Montgomeryville, PA, USA) in water at room temperature.

NIH-PA Author Manuscript

NIH-PA Author Manuscript

NIH-PA Author Manuscript

Results and Discussion

Absorption and fluorescence measurements

BSA Au_{25} nanoclusters were synthesized using an established protocol and were characterized for their absorption and fluorescence properties. In Figure 1, the red line shows the extinction spectrum of synthesized BSA Au_{25} clusters showing small bump around 500 nm. Due to particulate nature of the BSA Au_{25} clusters, it shows a distinct scattering component in their extinction spectrum.

In order to get the corrected absorbance, we measured the extinction in the range 850 nm – 300 nm. Since the absorption of clusters begins at about 600 nm, the spectral range 850 nm – 600 nm can be fitted with the Rayleigh scattering function ($1/\lambda^4$) and the appropriate Rayleigh scattering contribution can be subtracted at shorter wavelengths from the extinction spectrum of BSA Au_{25} clusters as shown by the dashed black line.

The blue line in Figure 1 shows the re-convoluted absorption spectrum of BSA Au_{25} clusters. This broad absorption spectrum (from 600 nm to 310 nm) is composed of multiple transitions showing a peak around 360nm and shoulder around 500nm. We resolved this spectrum assuming Gaussian distribution of transitions across the absorption spectrum.

Fluorescence excitation spectra of clusters show peaks around 330nm, 510nm and shoulder around 380nm (Figure 6). This information was used while Gaussian approximation of the absorption spectra to assign the peak values.

Figure 2 shows the BSA Au_{25} clusters absorption spectrum numerically decomposed to three Gaussian components that already gives a satisfactory fit to the experimental results. The significant overlap between absorption transitions fitted with Gaussians were further supported wavelength dependence of steady state anisotropy data which is discussed in section steady state anisotropy measurements. Jin et al have reported presence of three well defined bands in optical absorption spectra of thiol protected Au_{25} clusters [19].

The broad absorption spectrum of BSA Au_{25} clusters can be an indication for the presence of a size distribution that was further confirmed by measuring the hydrodynamic size using dynamic light scattering. The average particle size was found to be around 8 nm (Figure 2) with a narrow size distribution supporting the possibility of the presence of at least two BSA molecules holding gold cluster together. This observation is in well agreement with the report from Purkayastha *et al*[20].

The emission for BSA Au_{25} clusters has a maximum around 660 nm with a broad emission spectrum from 550 nm to 850 nm when excited at 470 nm. Different investigators report different emission peaks (from 640 nm to 710 nm) despite the use of a common synthesis protocol [21-23] This discrepancy may arise due to use of BSA from different manufacturing sources and impurities present in it. We have observed reproducibility in luminescence properties of BSA Au_{25} cluster after repeating the synthesis protocol at least 4 times. Figure 3 shows the emission spectra (corrected for absorbance at 515 nm) of rhodamine B and BSA Au_{25} clusters to provide a visual comparison of the quantum efficiency. The quantum yield of these clusters was found to be ~6 %.

Furthermore, we also looked at the fluorescence decay of BSA Au_{25} clusters as shown in Figure 4. It showed a heterogeneous decay which needed at least 3 exponential intensity decay components to fit the data. The average lifetime was 1.84 μs. We found distinct polarization behavior from these long lifetime BSA Au_{25} clusters.

NIH-PA Author Manuscript

NIH-PA Author Manuscript

NIH-PA Author Manuscript

Steady state anisotropy measurements

Figure 5, left vertical panels shows the excitation spectra and anisotropy spectra in glycerol, propylene glycol and water. In order to attain the limiting value, anisotropy was measured in glycerol at −20°C. We observed that, along the first transition (over the range of 320 nm to 450 nm) anisotropy was around 0.09 in glycerol, and after 450 nm there is a steady increase in the anisotropy to reach the limiting anisotropy of 0.35. In the case of propylene glycol it is 0.20, and 0.05 in water at 22°C owing depolarization due to a fast rotational diffusion compared to glycerol at −20°C. Anisotropy in low temperature glycerol is about 0.09 in the range of 320 nm to 450 nm which can be supported by our Gaussian approximation (Figure 2). Although we do not know the precise orientation of absorption transitions, overlap of multiple transitions in this spectral region (320 nm to 450 nm) leads to lower anisotropy values and it needs further work. As expected, the increase in anisotropy from 450 nm onwards supports our Gaussian approximation where the contribution from the 2nd Gaussian starts to decrease and anisotropy reaches the limiting value around 580 nm where the contribution from other transitions is none or negligible.

Figure 5, right side vertical panels shows the emission spectra and emission anisotropy spectra of BSA Au_{25} clusters in glycerol, propylene glycol and water using 590nm excitation. Since we are close to the limiting anisotropy at this excitation, the emission anisotropies were found to follow similar trends as excitation and decreased with decreasing solvent viscosity. Emission anisotropy for glycerol is 0.30, for propylene glycol 0.20 and slightly over zero in water. Emission anisotropy was constant throughout the emission spectrum in all the cases.

Time resolved anisotropy measurements

In case of water (Figure 6), fast motions in low viscosity solvent results in rapid anisotropy decay and faster correlation time. The anisotropy decays of BSA Au_{25} clusters in propylene glycol are shown in Figure 7. A slower motion and very slow decay in anisotropy was observed. Similar decay was observed when the same sample was excited using 550 nm wavelength while keeping the emission observation at 700 nm (Figure 7: lower panel), however the recovered r_0 value decreased significantly. This is in agreement with the excitation anisotropy data and shows the excitation dependence of the anisotropy. The rotational correlation times were same for both the decays in propylene glycol; however there is a change in the amplitudes of the two fractions. The recovered r_0 value 0.22 for propylene glycol and 0.2 for water are lower than the limiting anisotropy value (0.35) which indicates some initial anisotropy losses due to fast sub-nanosecond motions; however, dominant time dependant anisotropy changes are due to overall molecule rotations in nanoseconds range.

Conclusions

In this report we have synthesized the BSA Au_{25} clusters using the established protocol, and we have confirmed its absorption and emission properties. The major observation of our study is the presence of polarization behavior in these long fluorescence lifetime clusters. The presence of polarization properties among these clusters opens up a door to many exciting applications such as the study of large molecular weight protein complexes which would otherwise be difficult to study due to the absence of long fluorescence lifetime probes. Presence of long lifetime and anisotropy can be explored for time gated detection in microscopy and imaging. Moreover it can also be applied in developing anisotropy based bio and chemical sensing applications.

NIH-PA Author Manuscript

NIH-PA Author Manuscript

NIH-PA Author Manuscript

Supplementary Material

Refer to Web version on PubMed Central for supplementary material.

Acknowledgments

This work was supported by the NIH GRANT R01EB12003. We would like to thank Dr.J. Vishwanatha for letting us use particle size measurement instrument: Nanotrac system (Mircotrac, Inc., Montgomeryville, PA, USA)

Notes and references

1. Lu Y, Chen W. Chem. Soc. Rev. 2012; 41:3594–3623. [PubMed: 22441327]
2. Xu H, Suslick KS. Adv Mater. 2010; 22:1078–1082. [PubMed: 20401932]
3. Wang XX, Wu Q, Shan Z, Huang QM. Biosens. Bioelectron. 2011; 26:3614–3619. [PubMed: 21382705]
4. Fang YM, Song J, Li J, Wang YW, Yang HH, Sun JJ, Chen GN. Chem. Commun. (Camb). 2011; 47:2369–2371. [PubMed: 21165495]
5. Durgadas CV, Sharma CP, Sreenivasan K. Analyst. 2011; 136
6. Ma G, Binder A, Chi M, Liu C, Jin R, Jiang DE, Fan J, Dai S. Chem. Commun. (Camb). 2012
7. Qian H, Zhu M, Wu Z, Jin R. Acc. Chem. Res. 2012; 45:1470–1479. [PubMed: 22720781]
8. Wu Z, Wang M, Yang J, Zheng X, Cai W, Meng G, Qian H, Wang H, Jin R. Small. 2012; 8:2028–2035. [PubMed: 22488747]
9. Xie J, Zheng Y, Ying JY. J. Am. Chem. Soc. 2009; 131:888–889. [PubMed: 19123810]
10. Hu L, Han S, Parveen S, Yuan Y, Zhang L, Xu G. Biosens. Bioelectron. 2012; 32:297–299. [PubMed: 22209331]
11. Le Guevel X, Daum N, Schneider M. Nanotechnology. 2011; 22:275103. [PubMed: 21613679]
12. Zhou T, Huang Y, Li W, Cai Z, Luo F, Yang CJ, Chen X. Nanoscale. 2012; 4:5312–5315. [PubMed: 22837049]
13. Chen TH, Tseng WL. Small. 2012; 8:1912–1919. [PubMed: 22461355]
14. Sakanaga I, Inada M, Saitoh T, Kawasaki H, Iwasaki Y, Yamada T, Umezu I, Sugimura A. Applied Physics Express. 2011; 4:5001.
15. Wu Z, Jin R. Nano Lett. 2010; 10:2568–2573. [PubMed: 20550101]
16. Wen X, Yu P, Toh Y, Hsu A, Lee Y, Tang J. J.Phy.Chem. 2012; 116:19032–19038.
17. Wen X, Yu P, Toh Y, Hsu A, Tang J. J.Phy.Chem. 2012; 116:11830–11836.
18. López AF, Ruiz OP, López AI. J. Lumin. 1989; 44:105–112.
19. Zhu M, Aikens CM, Hollander FJ, Schatz GC, Jin R. J. Am. Chem. Soc. 2008; 130:5883–5885. [PubMed: 18407639]
20. Das T, Ghosh P, Shanavas MS, Maity A, Mondal S, Purkayastha P. Nanoscale. 2012; 4:6018–6024. [PubMed: 22915187]
21. Durgadas CV, Sharma CP, Sreenivasan K. Nanoscale. 2011; 3:4780–4787. [PubMed: 21956754]
22. Zhang A, Tu Y, Qin S, Li Y, Zhou J, Chen N, Lu Q, Zhang B. J. Colloid Interface Sci. 2012; 372:239–244. [PubMed: 22289255]
23. Wu X, He X, Wang K, Xie C, Zhou B, Qing Z. Nanoscale. 2010; 2:2244–2249. [PubMed: 20835443]

NIH-PA Author Manuscript

NIH-PA Author Manuscript

NIH-PA Author Manuscript

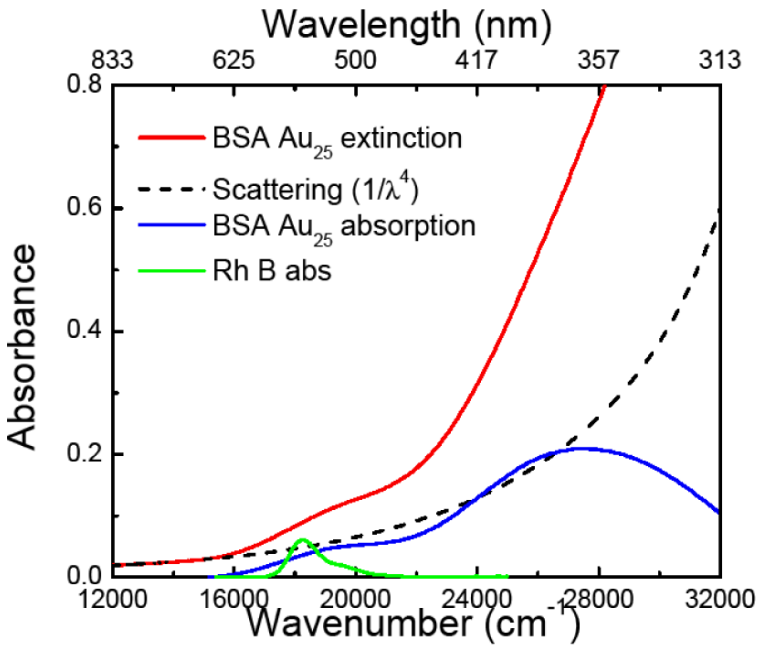

Fig. 1.

Extinction spectrum of synthesized BSA Au_{25} clusters (red line), scattering function (black dashed line) extrapolated from long wavelength spectrum of BSA Au_{25} cluster, corrected absorption after subtracting scattering function from extinction of BSA Au_{25} cluster (blue line) and rhodamine B absorption (green line).

NIH-PA Author Manuscript

NIH-PA Author Manuscript

NIH-PA Author Manuscript

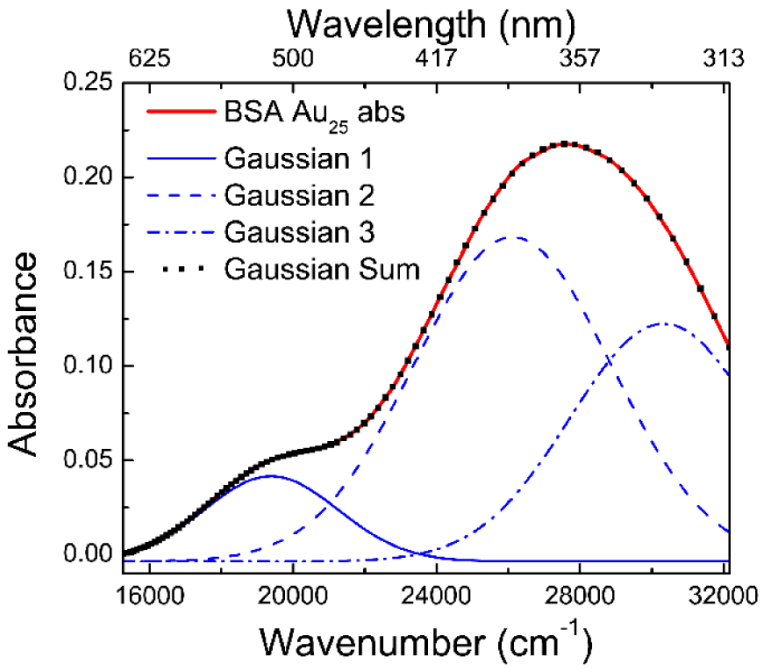

Fig.2.

Absorption spectrum of BSA Au_{25} approximated by three Gaussians. The square dotted spectrum is the best nonlinear least square fit to the three Gaussian components. The long wavelength transition significantly overlaps with the second strong band.

NIH-PA Author Manuscript

NIH-PA Author Manuscript

NIH-PA Author Manuscript

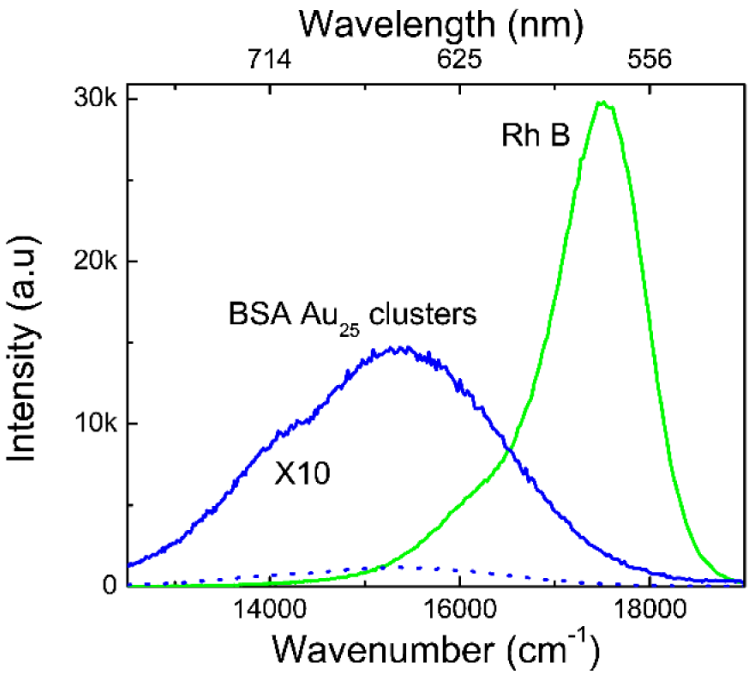

Fig.3.

Emission spectra of BSA Au_{25} and Rh B in ethanol when excited using 510 nm, scanned from 515 to 800 nm using 515 LP filter on emission side. Absorption of RhB at 510 nm was adjusted to the same value as absorption of the BSA Au_{25} cluster sample. The quantum efficiency of BSA Au_{25} clusters is about 6 %.

NIH-PA Author Manuscript

NIH-PA Author Manuscript

NIH-PA Author Manuscript

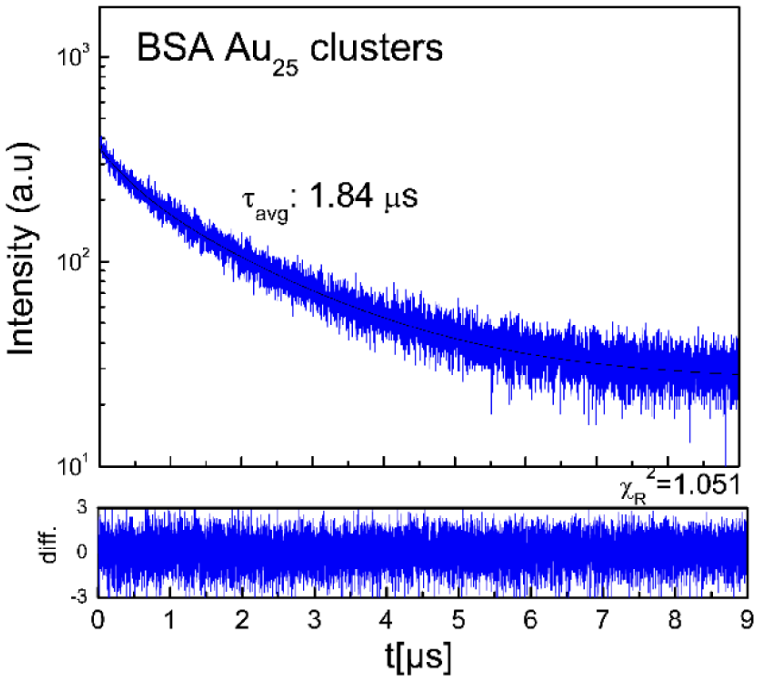

Fig.4.

Fluorescence intensity decay of BSA Au cluster in water (pH 6) at room temperature when excited at 470 nm. Emission intensity was observed at 660 nm. A three exponential model was used to fit the decay with lifetimes and amplitudes as: 1.88 μs (40.75%), 0.44 μs (19.27 %) and 0.009 μs (39.98 %).

NIH-PA Author Manuscript

NIH-PA Author Manuscript

NIH-PA Author Manuscript

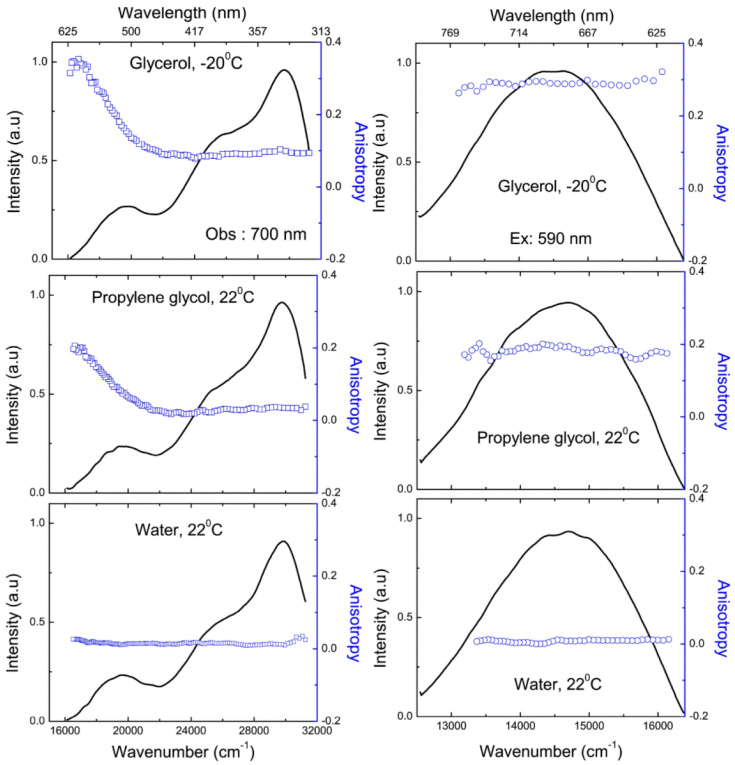

Fig.5.

Left vertical panels: Excitation spectra and excitation anisotropy spectra of BSA Au_{25} clusters in (top) glycerol, −20 deg C (middle) propylene glycol, 22 deg C and (bottom) DI Water, 22 deg C. Right vertical panels: Emission spectra and emission anisotropy spectra of BSA Au_{25} clusters in (top) glycerol, −20 deg C (middle) propylene glycol, 22 deg C and (bottom) DI Water, 22 deg C.

NIH-PA Author Manuscript

NIH-PA Author Manuscript

NIH-PA Author Manuscript

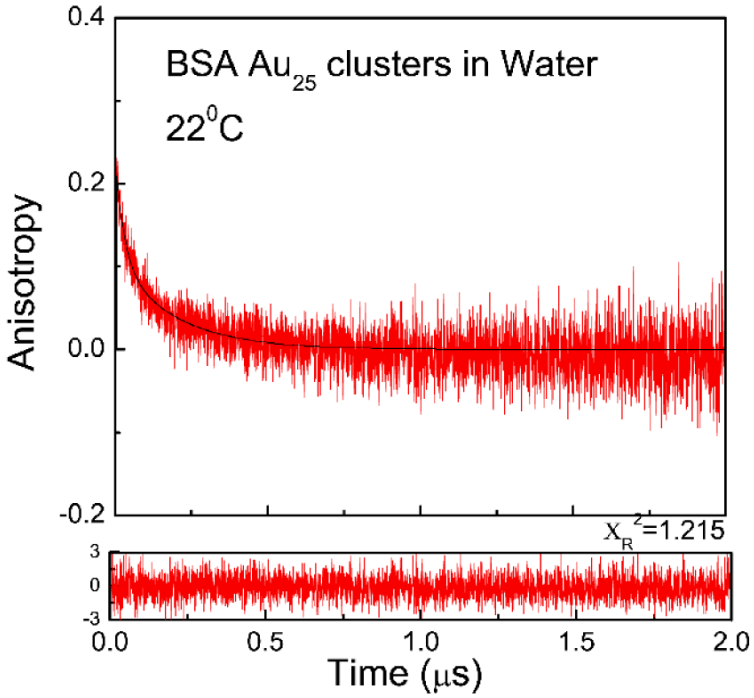

Fig.6.

Fluorescence anisotropy decay of BSA Au_{25} clusters in water at 600 nm excitation and 700 nm observation at 22°C. Recovered correlation times are Φ_1=0.029μs and Φ_2=0.195μs

NIH-PA Author Manuscript

NIH-PA Author Manuscript

NIH-PA Author Manuscript

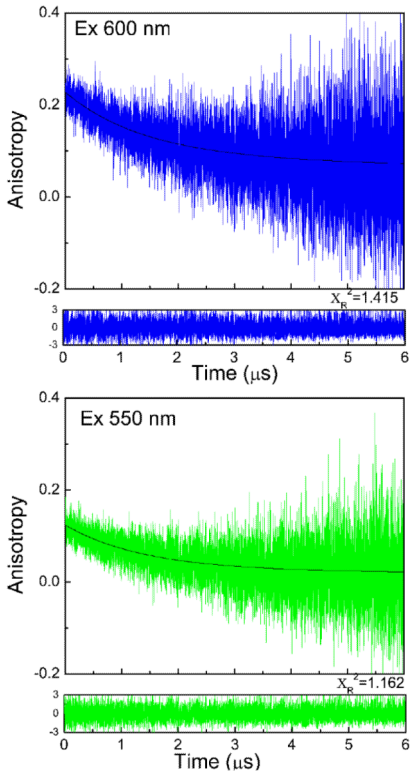

Fig.7.

Fluorescence anisotropy decays of BSA Au_{25} clusters in propylene glycol at 22°C. Upper panel: excitation at 600 nm and observation 700 nm and lower panel: excitation at 550 nm and observation 700 nm. Recovered correlation times are Φ_1=26.9μs and Φ_2=1.34μs in both cases.